Journal of Pathology
J Pathol 2019; **247:** 333–346
Published online 16 January 2019 in Wiley Online Library (wileyonlinelibrary.com) DOI: 10.1002/path.5193

ORIGINAL PAPER

Inflammation induces endothelial-to-mesenchymal transition and promotes vascular calcification through downregulation of BMPR2

Gonzalo Sánchez-Duffhues[1]*, Amaya García de Vinuesa[1], Vera van de Pol[1], Marlieke E Geerts[2], Margreet R de Vries[2], Stef GT Janson[1], Hans van Dam[1], Jan H. Lindeman[2], Marie-José Goumans[1] and Peter ten Dijke[1]

[1] *Department of Cell and Chemical Biology, Oncode Institute, Leiden University Medical Center, Leiden, The Netherlands*
[2] *Department of Vascular Surgery, Leiden University Medical Center, Leiden, The Netherlands*

**Correspondence to: G Sánchez-Duffhues, Department of Cell and Chemical Biology (Room R2-20), Leiden University Medical Center, Postzone S-1-P, postbus 9600, 2300RC Leiden, The Netherlands. E-mail: g.sanchez_duffhues@lumc.nl*

Abstract

Endothelial-to-mesenchymal transition (EndMT) has been unveiled as a common cause for a multitude of human pathologies, including cancer and cardiovascular disease. Vascular calcification is a risk factor for ischemic vascular disorders and slowing calcification may reduce mortality in affected patients. The absence of early biomarkers hampers the identification of patients at risk. EndMT and vascular calcification are induced upon cooperation between distinct stimuli, including inflammatory cytokines and transforming growth factor beta (TGF-β) family members. However, how these signaling pathways interplay to promote cell differentiation and eventually vascular calcification is not well understood. Using *in vitro* and *ex vivo* analysis in animal models and patient-derived tissues, we have identified that the pro-inflammatory cytokines tumor necrosis factor alpha (TNF-α) and interleukin-1 beta (IL-1β) induce EndMT in human primary aortic endothelial cells, thereby sensitizing them for BMP-9-induced osteogenic differentiation. Downregulation of the BMP type II receptor BMPR2 is a key event in this process. Rather than compromising BMP canonical signal transduction, loss of BMPR2 results in decreased JNK signaling in ECs, thus enhancing BMP-9-induced mineralization. Altogether, our results point at the BMPR2–JNK signaling axis as a key pathway regulating inflammation-induced EndMT and contributing to calcification.

Keywords: bone morphogenetic protein; vascular calcification; c-Jun N-terminal kinase; endothelial cell; endothelial-to-mesenchymal transition; fibroblast; inflammation; osteoblast; transforming growth factor beta; tumor necrosis factor alpha; pulmonary arterial hypertension

Received 24 April 2018; Revised 4 October 2018; Accepted 30 October 2018

No conflicts of interest were declared.

Introduction

Vascular calcification is a prevalent feature in cardiovascular diseases associated with elevated risk of mortality. The underlying cellular and molecular mechanisms involved have been an area of intense study in recent decades. Mineralization of blood vessels occurs through a coordinated crosstalk between different cell types and cytokines, but ultimately relies on osteoblast lineage cells for synthesis and mineralization of the calcified matrix [1]. We and others have shown that endothelial cells (ECs) can function as an additional source of osteogenic progenitors in vascular calcification [2–4]. ECs can undergo a process known as endothelial-to-mesenchymal transition (EndMT), which involves loss of endothelial features and acquisition of a fibroblast-like phenotype, eventually leading to cells with osteogenic potential. EndMT is modulated by different extracellular growth factors [transforming growth factor beta (TGF-β) family ligands, inflammatory cytokines, fibroblast growth factors] and conditions (mechanical stress, hypoxia) (reviewed in ref [5]). During the onset and progression of calcified plaques in the aorta, both inflammatory cytokines [such as tumor necrosis factor alpha (TNF-α) and interleukin-1 beta (IL-1β) [6]] and TGF-β family ligands [including the bone morphogenetic proteins (BMPs) [7,8]) coincide in the affected area. Whereas BMP-2 and BMP-4 mainly have a paracrine function, BMP-9 and BMP-6 are found in the systemic circulation [9]. BMP-9 regulates vascular homeostasis by controlling proliferation [10], angiogenesis [11], permeability [12] and monocyte recruitment [13]. Interestingly, BMP-9 induces heterotopic ossification when expressed ectopically using adenovirus [14]. Importantly, administration of BMP antagonists prevents experimental

atherosclerosis in preclinical animal models [15,16], highlighting the relevance of this pathway in the context of atherosclerosis.

TGF-β signaling is initiated with the oligomerization of receptor complexes at the cell membrane upon ligand binding. BMPs signal via complexes consisting of a type I receptor named activin receptor-like kinase (ALK)1/2/3/6, and one of three possible type II receptors: BMPR2, activin type II receptor A, or activin type II receptor B (ACVR2A, ACVR2B) [17]. Receptor activation induces the phosphorylation of SMAD1/5/8, which form heteromeric complexes with SMAD4 and translocate into the nucleus to regulate gene expression. In osteogenic cells, BMPs induce the transcription of genes related to osteoblast differentiation and activation [18]. In addition to this so-called canonical SMAD signaling pathway, TGF-β family ligands modulate the activity of different mitogen-activated protein (MAP) kinases, including ERK (extracellular signal-regulated kinase), p38, and JNK (c-Jun N-terminal protein kinase) in a cell-specific and context-dependent fashion [19,20]. Furthermore, how BMP signaling is fine-tuned by inflammation in EndMT-derived cells and cells with osteogenic potential is yet to be determined. Whereas some have suggested that inflammatory stimuli inhibit BMP signaling and osteoblast differentiation and activation [21,22], others have shown that inflammation is needed for osteogenesis [23,24].

In this study, we investigated the interplay between inflammation and BMP signaling in ECs. We found that TNF-α and IL-1β induce EndMT in primary ECs, which become prone to undergo osteogenic differentiation in response to BMP-9. We identified BMPR2 downregulation as a key event in this process, which leads to decreased JNK activation, thereby enhancing BMP-9-induced mineralization. Finally, we supported our findings in a preclinical animal model of atherogenesis, as well as patient-derived tissues from atherosclerotic donors. Our results provide a better understanding of the molecular mechanisms underlying EndMT and vascular calcification, and may have broad implications for other human inflammatory pathologies involving BMP signaling.

Materials and methods

Cell culture and reagents

Human aortic endothelial cells (HAoECs, CC-2535, Batch number 0000316662), pulmonary aortic endothelial cells (PAECs, CC-2530), and coronary microvascular endothelial cells (cMVECs, CC-7030) were purchased from Lonza (Walkerville, MD, USA). Human skin microvascular endothelial cells (HMECs) have been described elsewhere [25]. All cells were cultured in complete EBM-2 medium (Lonza) on 1% w/v gelatin-coated wells. Endothelial colony-forming cells (ECFCs) were isolated as previously described [26] and cultured in complete EBM-2 medium. All experiments were performed with cells grown to near-confluency between passage 6 and 8. 2H-11 cells are derived from endothelial cells isolated from the lymph nodes of adult C3H/HeJ mice transformed using SV40 [27,28]. These cells were grown on 1% w/v gelatin-coated dishes (Merck, Darmstadt, Germany) in DMEM medium (Invitrogen, Breda, The Netherlands) supplemented with 4.5 g/l D-glucose, 110 mg/l sodium pyruvate, non-essential amino acids (all from Invitrogen), 10% (v/v) heat-inactivated fetal bovine serum (FBS; Sigma-Aldrich Chemie, Steinheim, Germany), 0.5% (v/v) antibiotic/antimyotic solution (Invitrogen), and 2 mM L-glutamine (Invitrogen).

EndMT assays

HAoECs were seeded at confluence in 12-well plates (for qPCR) or Lab-Tek II chamber slides (for immunofluorescence) in EBM2 complete medium containing 2% FBS. Next day, the cells were stimulated with the indicated ligands for 24 h in EBM2 complete medium containing 10% FBS, and endothelial and mesenchymal-specific markers were analyzed by RT-qPCR or immunofluorescent labeling.

Osteoblast differentiation assays

Formation of calcium and phosphate deposits was analyzed by Alizarin Red staining (ARS) of cells seeded in 48-well plates at near-confluency. HAoECs were pretreated with TNF-α (10 ng/ml) or TGF-β_3 (5 ng/ml) for 4 days in EBM2 containing 10% FBS. Next, the medium was replaced by osteogenic medium (DMEM containing 10% FBS, 10^{-8} mol/l dexamethasone, 0.2 mmol/l ascorbic acid, and 10 mmol/l β-glycerolphosphate) in the presence of BMP-9 (10 ng/ml) for 14 days. 2H-11 cells were incubated with the aforementioned osteogenic medium containing both TNF-α (10 ng/ml) and BMP-9 (10 ng/ml) for 14 days. The medium was refreshed every 4 days. Afterwards, cells were washed twice with PBS and fixed with 3.7% formaldehyde for 5 min, washed twice with distilled water, and ARS was performed as previously described [29]. Precipitates from three independent assays were dissolved using 10% cetylpyridinium chloride and absorbance was measured at 570 nm. Representative pictures were obtained using a Leica DMIL LED microscope with 10× magnification.

Reverse transcription–quantitative PCR

Total RNA was extracted using NucleoSpin RNA II (MACHEREY-NAGEL, Duren, Germany), 500 ng of RNA were reverse transcribed using RevertAid First Strand cDNA Synthesis Kits (Fermentas/Thermo Fisher Scientific, Freemont, CA, USA) and quantitative PCR (qPCR) was performed using SYBR Green (Bio-Rad, Veenendaal, The Netherlands) and a Bio-Rad CFX Connect. The primers used are listed in the supplementary material, Supplementary materials and methods. *GAPDH* was used for normalization.

Immunofluorescent labeling of cultured cells

HAoECs grown on coverslips were fixed with 4% formaldehyde for 30 min at room temperature, washed with glycine for 5 min, permeabilized with 0.2% Triton X-100, and blocked in PBS containing 5% BSA for 1 h. The cells were incubated overnight at 4°C with primary antibody in blocking solution with gentle shaking. Next day, the cells were washed five times in washing buffer (PBS containing 0.05% Tween-20 and 1% BSA) and incubated with secondary antibody (Alexa-Fluor FITC goat anti-mouse IgG, Alexa-Fluor 555 anti-rabbit IgG; Invitrogen; 1:200) or with phalloidin-488 (1:100) in PBS with 0.5% BSA for 1 h. Finally, the cells were washed five times in washing buffer and mounted in Prolong Gold containing DAPI (Invitrogen). Preparations were imaged in a Leica SP5 confocal scanning laser microscope. A representative picture from each staining is shown ($n = 3$). The antibodies used are described in the supplementary material, Supplementary materials and methods.

Western blotting

The cells were seeded into 12-well plates and cultured until they reached confluence. Next, the cells were stimulated as indicated, washed with cold PBS, and lysed in 2× sample buffer as previously described [30]. The protocol details and the antibodies used are provided in the supplementary material, Supplementary materials and methods.

Lentiviral production and transduction

Lentiviral vectors were produced in HEK293T cells as previously described [29]. Lentiviral vectors expressing specific shRNAs were obtained from Sigma (MISSION® shRNA; see supplementary materials and methods). Lentiviral vectors to overexpress mMKP-1 have been described elsewhere [31].

Vein graft procedure

Vein grafts were performed as reported elsewhere [32]. Details may be found in the supplementary material, Supplementary materials and methods.

Immunostaining of tissues

Immunofluorescent and immunohistochemical staining on human and murine aortic tissues was performed as previously described [3] (see the supplementary material, Supplementary materials and methods for details). Human aortic sections (4 μm) were prepared from each donor and classified according to the revised classification of the American Heart Association (AHA) [33,34] by two independent observers with no knowledge of the donor characteristics. Sample collection and handling were performed in accordance with the guidelines of the Medical and Ethical Committee in Leiden, The Netherlands and the code of conduct of the Dutch Federation of Biomedical Scientific Societies.

Transfections, luciferase assays, and DNA constructs

For luciferase reporter assays, the cells were seeded in 24-well plates and transfected with DharmaFECT Duo (Thermo Fisher Scientific) following the recommendations of the manufacturer. The cells were harvested and lysed 48 h after transfection. Luciferase activity was measured using the luciferase reporter assay system from Promega (Leiden, The Netherlands) by a Perkin Elmer luminometer Victor^3 1420. Each transfection mixture was equalized with empty vector when necessary and experiments were performed in triplicate. The BRE-Luc reporter is reported elsewhere [35]. The expression vector encoding the constitutively active fusion protein MKK7–JNK3 and its characterization have been described previously [36].

Iodination and ligand affinity labeling of cell surface receptors

Iodination of BMP-9 was performed according to the chloramine T method and cells were subsequently affinity labeled with the radioactive ligand as previously described [37]. Cell lysates were immunoprecipitated with antibodies against ALK1, ALK2, BMPR2, and ACVR2A. The generation and characterization of these antibodies have been published previously [38–40]. Image quantification was performed by densitometry using ImageJ analysis.

Statistical analysis

All experiments were performed at least three times; results are shown as mean ± SD. Student's *t*-test was used for statistical analysis, and $^{+,*}p < 0.05$, $^{++,**}p < 0.01$, $^{+++,***}p < 0.001$ were considered significant. Representative data are shown in the figures.

Results

TNF-α and IL-1β induce EndMT in HAoECs, thereby enhancing BMP-induced mineralization

To determine the mechanisms by which ECs contribute to the generation of atherosclerotic plaques, we used primary human coronary aortic endothelial cells (HAoECs) stimulated with the indicated pro-inflammatory cytokines and members of the TGF-β superfamily of growth factors. After 24 h, TNF-α and IL-1β induced a decrease in the endothelial markers *CDH5* (encoding for VE-cadherin) and *PECAM1*, and an upregulation of the mesenchymal genes *CDH2* (encoding for N-cadherin) and *FN1* (fibronectin) (Figure 1A). Accordingly, these two cytokines upregulated the expression of *SNAI1* and *TWIST1* (supplementary material, Figure S1). This correlated with loss of the typical endothelial cobblestone-like phenotype, seen by cytoskeletal staining with phalloidin, and the downregulation of VE-cadherin, PECAM-1, and TIE2, and increase in N-cadherin, αSMA, and vimentin (Figure

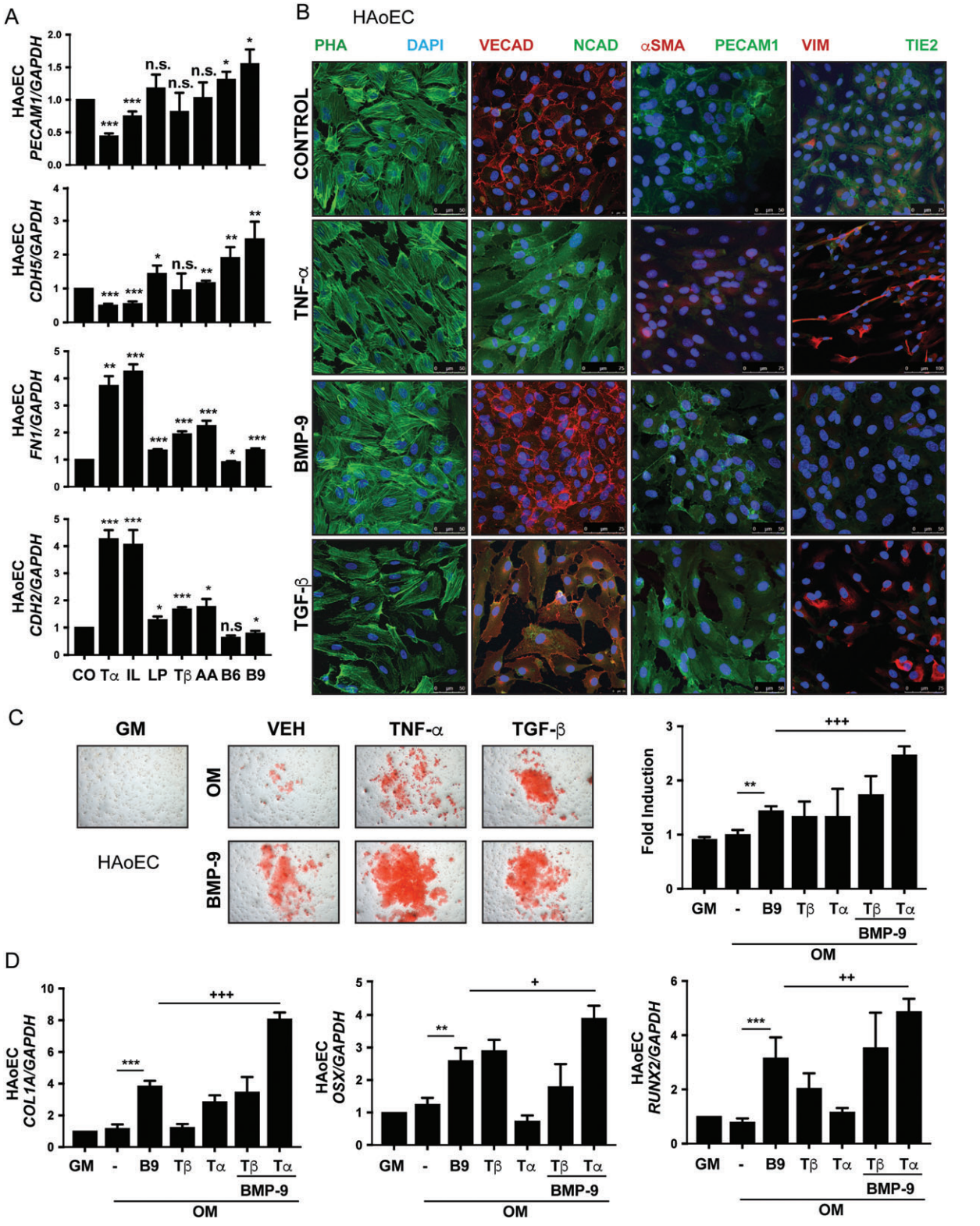

Figure 1. The pro-inflammatory cytokine TNF-α induces EndMT in HAoECs, priming them for BMP-9-induced osteogenic differentiation. (A) Gene expression analysis of *CDH5*, *PECAM1*, *FN1*, and *CDH2* in HAoECs stimulated for 24 h with the indicated cytokines and growth factors. CO: control; Tα: TNF-α (10 ng/ml); IL: IL-1β (10 ng/ml); LP: LPS (10 ng/ml); Tβ: TGF-β_3 (5 ng/ml); AA: activin A (50 ng/ml); B6: BMP-6 (50 ng/ml); B9: BMP-9 (10 ng/ml). Statistical significant difference with respect to control cells (*, **, ***, n.s non significant). (B) Fluorescence staining of HAoECs stimulated with TNF-α, BMP-9 or TGF-β as above: PHA (phalloidin), VECAD (VE-cadherin), NCAD (N-cadherin), αSMA, PECAM1, VIM (vimentin), and TIE2. DAPI (blue) was used as a nuclear counterstain. (C) Alizarin Red staining and corresponding quantification on HAoECs incubated with BMP-9 for 21 days under osteogenic conditions after induction of EndMT with TNF-α or TGF-β. GM: growth medium; OM: osteogenic medium. Quantification is shown on the right side. Statistical significant difference with respect to untreated (**) or BMP-9 (+++) treated cells. (D) qPCR of the indicated osteogenic genes in HAoECs subjected to osteogenic differentiation. Statistical significant difference with respect to untreated (**, ***) or BMP-9 (+, ++, +++) treated cells.

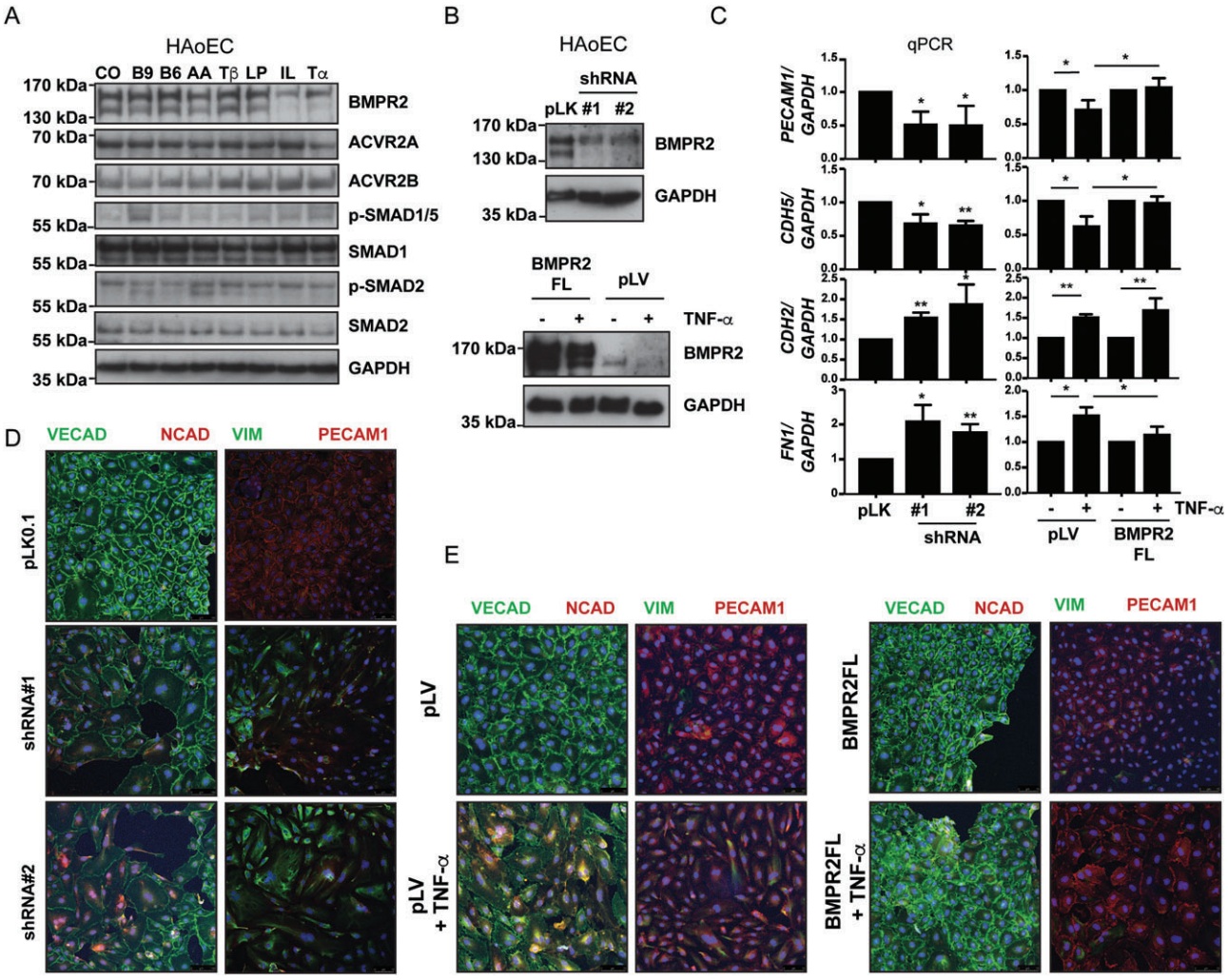

Figure 2. TNF-α-induced downregulation of BMPR2 is necessary for HAoECs to undergo EndMT. (A) Western blot in HAoECs where EndMT has been induced for 24 h (see Figure 1A,B). (B) Western blot in HAoECs transduced with control (pLK) lentivirus or two shRNA constructs (#1 and #2) against BMPR2 (upper panel) or with lentivirus encoding a full-length version of BMPR2 (BMPR2 FL) and treated with TNF-α for 24 h (lower panel). (C–E) EndMT analysis by (C) qPCR and (D, E) immunofluorescent staining in HAoECs knocked down for BMPR2 or overexpressing BMPR2 FL, respectively. Statistical significant difference with respect to control or TNF-α-treated cells (*, **).

1B). Furthermore, pretreatment with TNF-α sensitized HAoECs to become osteoblast-like cells in response to BMP-9, more potently than TGF-β, as shown by ARS (Figure 1C) and enhanced levels of the osteogenic genes *COL1A1* (collagen 1 alpha 1), *RUNX2*, and *OSX* (osterix/transcription factor Sp7) (Figure 1D). TNF-α alone induced *BMP7*, and the combination of BMP-9 and TNF-α upregulated osteogenic *BMP2* and *BMP4* (supplementary material, Figure S2). These results show that the pro-inflammatory cytokine TNF-α induces EndMT in HAoECs and that EndMT-derived cells exhibit an enhanced osteogenic response to BMP-9.

BMPR2 downregulation is necessary and sufficient for TNF-α to induce EndMT in HAoECs

BMP-9 signaling in ECs is mediated by two possible type I receptors, ALK1 and ALK2, and three type II receptors, BMPR2, ACVR2A, and ACVR2B [41]. We investigated whether the expression of the BMP type II receptors is modified by stimuli inducing EndMT, thereby enhancing the osteogenic response of BMP-9. The two potent inducers of EndMT, TNF-α and IL-1β, triggered a clear downregulation of BMPR2, whereas ACVR2A and ACVR2B were not affected (Figure 2A). This effect correlated with a decreased mRNA level of *BMPR2* (supplementary material, Figure S3) and was not exclusive to HAoECs, as endothelial colony-forming cells (ECFCs) and, to a lesser extent, human skin microvascular ECs (HMECs), displayed a similar response (supplementary material, Figure S4). Noteworthy, incubation with higher concentrations of TNF-α led to reduced expression of all three BMP type II receptors (supplementary material, Figure S5).

We next investigated whether BMPR2 downregulation is necessary for TNF-α to induce EndMT in HAoECs, using knockdown and overexpression experiments (Figure 2B). Knockdown of *BMPR2* in HAoECs using two different shRNA constructs resulted in reduced *CDH5* and *PECAM1*, and increased *CDH2* and *FN1* mRNA levels and loss of endothelial morphology.

In contrast, ectopic overexpression of a full-length BMPR2 construct (BMPR2 FL) in HAoECs using lentiviral particles prior to TNF-α stimulation prevented TNF-α-induced EndMT, shown by gene expression analysis (Figure 2C) and immunofluorescence (Figure 2D,E). Altogether, our results show that downregulation of BMPR2 is required for TNF-α to induce EndMT in HAoECs, and that BMPR2 overexpression can partially prevent EndMT.

BMPR2 is downregulated in ApoE3Leiden mice in response to a high-fat diet

We next aimed to validate our findings *in vivo* using an animal model of atherosclerosis. The contribution of EndMT to vascular calcification and atherosclerosis has been investigated in different animal models, including LDLR$^{-/-}$, ApoE-deficient, and Ins^{Akita} mice [4,42,43]. The ApoE3Leiden mice constitute a valuable model of diet-induced atherosclerosis with a human-like lipoprotein profile when fed a high-fat diet [30,39]. Furthermore, this model is currently considered as one of the models of native atherosclerosis closest to human pathology. Although some aspects of this model have already been characterized (e.g. a strong inflammatory infiltrate potentiates plaque development), the contribution of EndMT to plaque formation is not known. Therefore, we performed immunofluorescent co-staining for PECAM-1 and αSMA on sections from control animals (7 days normal diet vein grafts) and high hypercholesterolemic diet (high-fat diet, HFD)-induced atherosclerosis animals (after 7, 14, and 28 days). As previously reported [32], the luminal endothelial layer of the aorta of HFD mice downregulated PECAM-1 after 7 days, in contrast to control animals (Figure 3A, low magnification). This was accompanied by evident neointimal thickening. Interestingly, we observed PECAM-1 and αSMA double-positive cells migrating from the luminal layer into the neointima area (Figure 3A, high magnification). This phenomenon was visible from day 7 to day 28 in HFD animals, with a progressive increase of αSMA in the neointima. Consistent with our *in vitro* findings, BMPR2 was markedly reduced in the aorta at the onset of atherosclerosis, as early as 7 days after administration of HFD (Figure 3B).

Downregulation of BMPR2 does not compromise BMP-induced canonical SMAD1/5 signaling

To investigate the mechanisms by which loss of BMPR2 induced by TNF-α enhanced the osteogenic differentiation of ECs in response to BMP-9, we characterized an easy-to-culture EC line, 2H-11 murine ECs. First, we demonstrated that BMP-2, BMP-6, BMP-7, and BMP-9 induce cell calcification in 2H-11 cells (supplementary material, Figure S6A), which can be blocked by co-incubation with a BMP type I receptor kinase inhibitor (supplementary material, Figure S6B). Moreover, similar to primary HAoECs, knockdown of *Bmpr2* (but not *Acvr2A* or *Acvr2B*) enhanced the osteogenic differentiation of 2H-11 cells induced by BMP-9 (supplementary material, Figures S7 and S8). On the contrary, stable overexpression of *BMPR2* FL partially prevented the osteogenic effect of BMP-9 (supplementary material, Figure S9). Since one of the main determinants of osteogenic differentiation is the induction of BMP canonical SMAD1/5 signal transduction, we first analyzed whether this was affected by TNF-α. Although TNF-α pretreatment resulted in a dose-dependent increase in osteogenic differentiation of BMP-9-induced 2H-11 cells (Figure 4A), the canonical BMP-9-induced transcriptional response (as measured using the BRE-LUC reporter construct, Figure 4B) was not increased by TNF-α. Using a previously reported protocol for iodination and ligand affinity labeling of cell surface receptors, we studied the high affinity receptors for BMP-9 in 2H-11 cells. As Figure 4C shows, while BMP-9 mainly forms a receptor complex including BMPR2 in control conditions, upon *BMPR2* knockdown, BMP-9 recruits ACVR2A in a receptor signaling complex, together with ALK1/2 (supplementary material, Figure S10). To investigate whether this affects the canonical signaling response to BMP-9 in 2H-11 cells, we performed western blotting in stably knocked down 2H-11 cells for *Bmpr2*, *Acvr2A* or *Acvr2B*. As expected, single knockdown of any of the type II receptors failed to compromise the BMP-9-induced p-SMAD1/5 response. Interestingly, pretreatment with TNF-α blocked p-SMAD1/5 activation exclusively in cells knocked down for ACVR2A (Figure 4D). These results suggest that loss of BMPR2 induced by TNF-α leads to enhanced recruitment of ACVR2A in the signaling receptor complex to balance downstream canonical signaling in ECs.

Downregulation of BMPR2 decreases JNK pathway activation to fine-tune EC mineralization

Since the enhanced osteogenic response to BMP-9 of ECs lacking BMPR2 was not related to BMP-9 canonical signaling, we tested the effect of chemical inhibitors of non-canonical signaling on BMP-9-induced osteogenic differentiation. We used SP600125 to inhibit JNK, UO120 against ERK, SB203580 for p38 kinase, and PDTC (ammonium pyrrolidinedithiocarbamate) to block nuclear factor kappa B (NF-κB) signaling. Among all the inhibitors used, only SP600125 enhanced the osteogenic differentiation of 2H-11 cells (Figure 5A). We confirmed this using a mutant version of the phosphatase MKP-1 (mMKP-1) [31]. 2H-11 cells transduced with mMKP-1 showed decreased phosphorylation of c-Jun (p-c-Jun), a downstream target of JNK, in response to BMP-9 (supplementary material, Figure S11). Next, we investigated p-c-Jun in 2H-11 cells stably knocked down for BMPR2 or the other type II receptors. Downregulation of BMPR2, but not ACVR2A or ACVR2B, by two different shRNA constructs decreased p-c-Jun in response to BMP-9 (Figure 5B). Furthermore, chemical inhibition of JNK in shBMPR2 2H-11 cells failed to enhance the calcifying effect of BMP-9, unlike control (pLK0.1), shACVR2A,

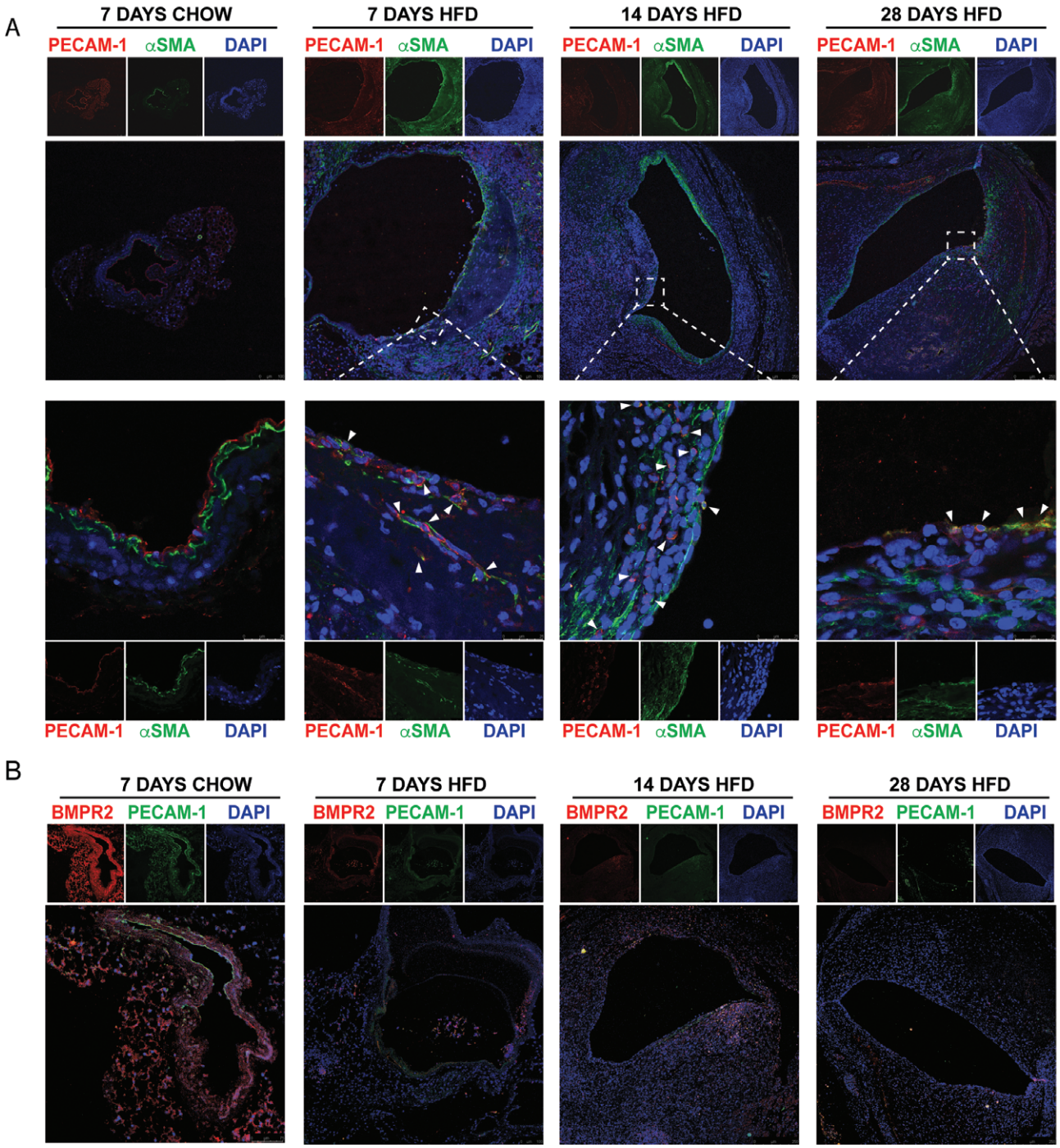

Figure 3. BMPR2 is downregulated in the aorta of ApoE3Leiden mice developing atherosclerotic disease. Aortic sections from ApoE3Leiden mice fed with a normal (Chow) or a high-fat diet (HFD) for 7, 14 or 28 days and stained for PECAM-1 and αSMA (A) or BMPR2 and PECAM-1 (B). A representative picture per condition is shown, including zoomed areas indicated in dashed lines. White arrows indicate PECAM-1/αSMA double-positive cells, suggestive of EndMT.

and shACVR2B stable cells (Figure 5C). This might suggest that BMPR2 functionally interacts with JNK to activate JNK signaling, as previously suggested [44,45]. Accordingly, endogenous JNK was detected in GST pull-down experiments performed with GST-BMPR2 (supplementary material, Figure S12). Finally, to determine the contribution of JNK signaling to the osteogenic differentiation of 2H-11 cells, we restored JNK signaling in cells with stable knockdown of *BMPR2* by overexpressing the MKK7-JNK3 fusion protein, which induces constitutive activation of JNK [36]. Ectopic overexpression of MKK7–JNK3 increased the levels of p-c-Jun (supplementary material, Figure S13). Interestingly, this correlated with partial inhibition of BMP-9-induced mineralization (Figure 5D). Taken together, these data confirm that downregulation of JNK activity in ECs favors their osteogenic differentiation in response to BMPs.

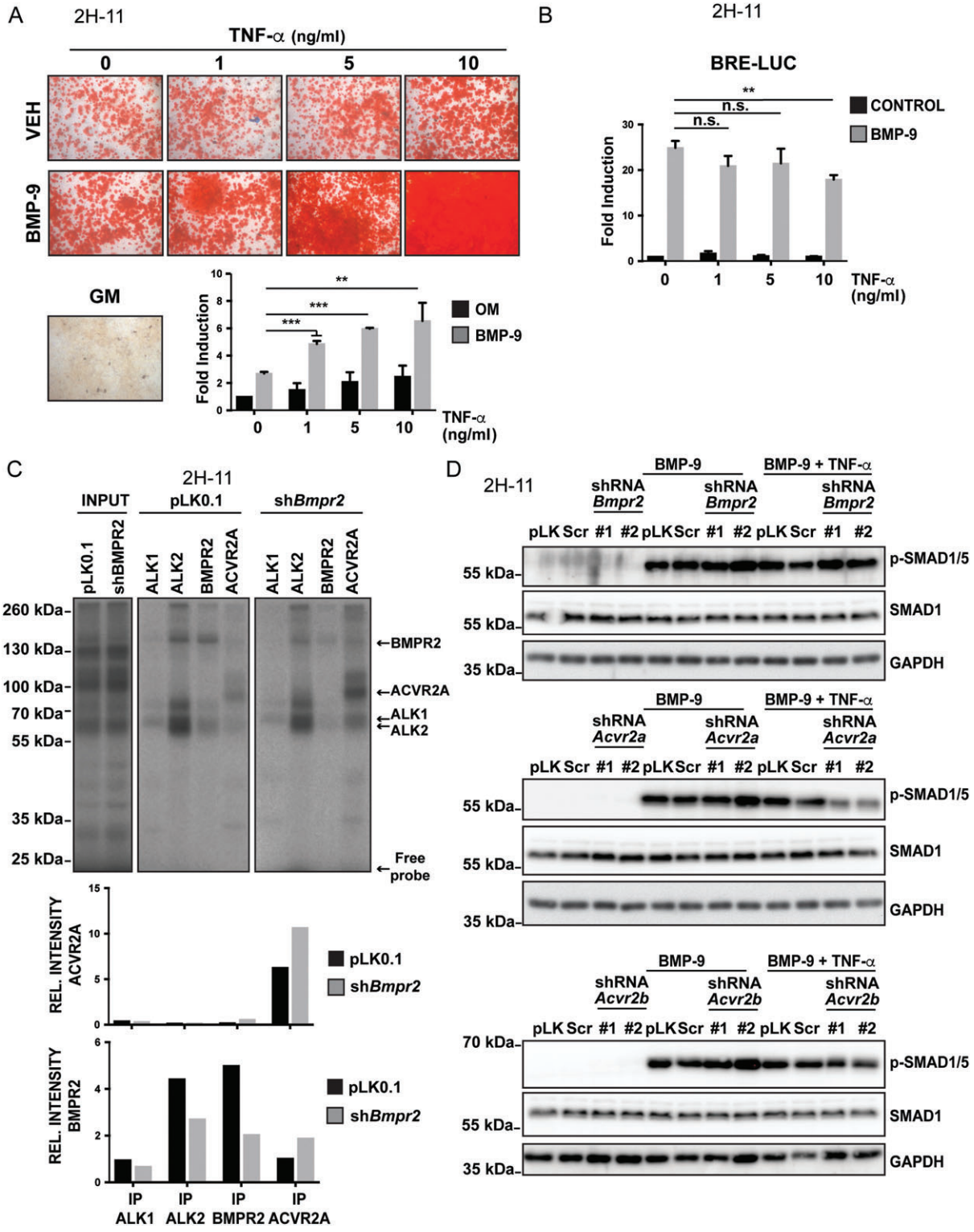

Figure 4. TNF-α-induced loss of BMPR2 does not compromise BMP-9 canonical signaling in ECs. (A) Alizarin Red staining and quantification (lower figure) in 2H-11 cells incubated with BMP-9 (10 ng/ml) and increasing concentrations of TNF-α. GM: growth medium. Statistical significant difference with respect to control or BMP-9/TNF-α-treated cells (**, *** or non significant). (B) BMP-9-induced canonical transcriptional response in 2H-11 cells stimulated with BMP-9 (10 ng/ml) upon pre-incubation with TNF-α. Fold induction of untreated control cells is shown. (C) Ligand–receptor interaction assay in 2H-11 cells stably knocked down for BMPR2 or a control vector (pLK0.1). Quantification is shown below. (D) Western blot of p-SMAD1/5 and total SMAD1 in 2H-11 cells stably knocked down for *Bmpr2*, *Acvr2A* or *Acvr2B* and treated with BMP-9 (10 ng/ml) and TNF-α (10 ng/ml).

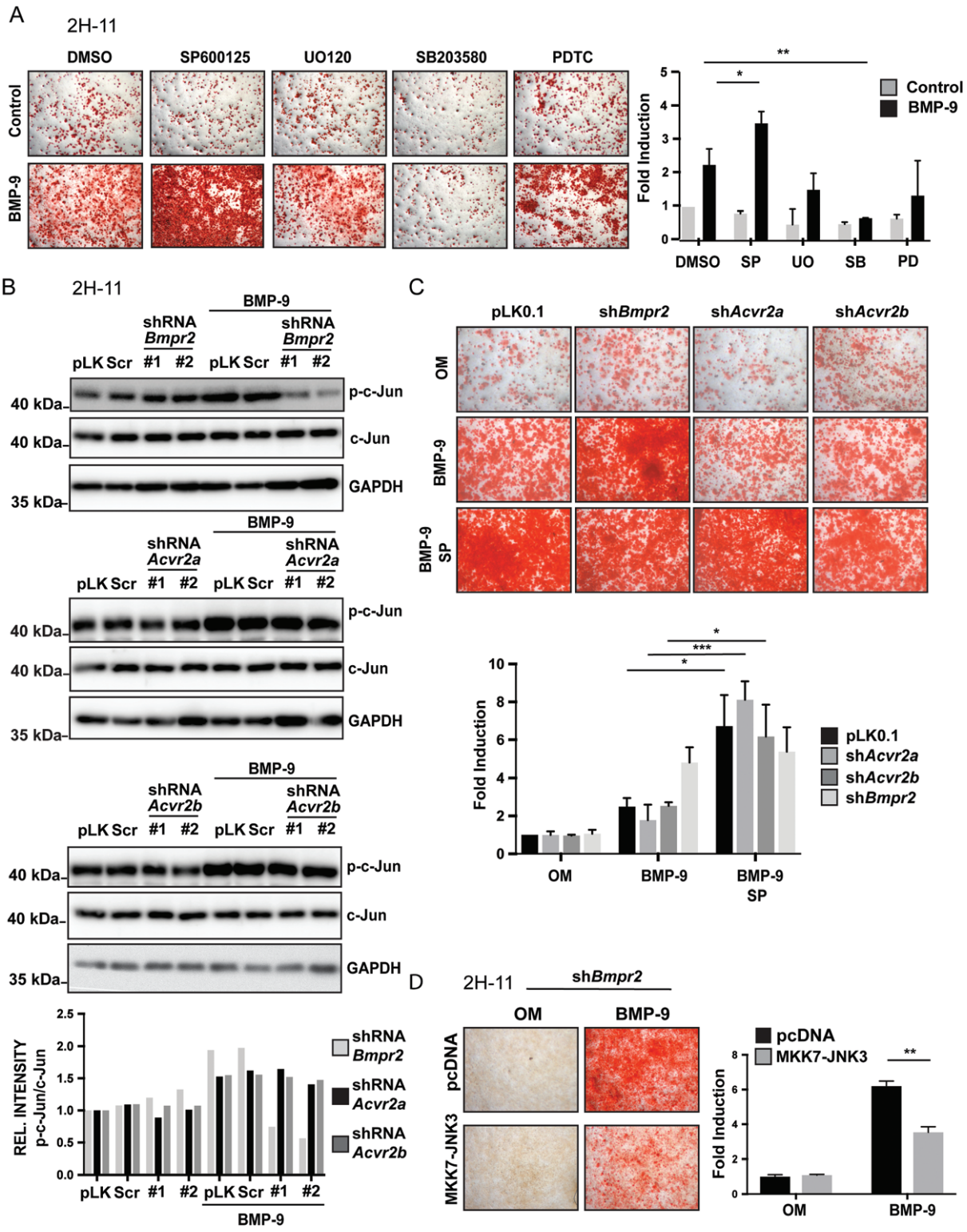

Figure 5. Loss of BMPR2 decreases c-Jun activation, thereby enhancing BMP-9-induced osteogenic differentiation of ECs. (A) Alizarin Red staining and quantification on 2H-11 cells co-treated for 14 days with BMP-9 (10 ng/ml) and chemical inhibitors targeting the JNK (SP600125, 5 μmol/l), ERK (UO120, 10 μmol/l), p38 (SB203580, 10 μmol/l), and NF-κB (PDTC, 50 μmol/l) signaling pathways, incubated under osteogenic conditions. Fold induction of DMSO-treated control cells is shown. (B) Western blot of p-c-Jun and total c-Jun in 2H-11 cells stably knocked down for *Bmpr2*, *Acvr2A* or *Acvr2B* and stimulated with BMP-9 (10 ng/ml) for 45 min. Quantification is shown below. (C) ARS staining and quantification on 2H-11 cells stably knocked down for *Bmpr2* (shRNA #1), *Acvr2A* (shRNA #1) or *Acvr2B* (shRNA #1) and stimulated for 14 days with BMP-9 (10 ng/ml) or BMP-9 and SP600125 (5 μmol/l) in osteogenic conditions. OM: osteogenic medium. (D) ARS staining and quantification in 2H-11 cells stably knocked down for *Bmpr2* and transfected with MKK7-JNK3 or an empty vector (pcDNA3), incubated with BMP-9 (10 ng/ml) under osteogenic conditions. Fold induction of pcDNA-transfected untreated cells is shown. OM: osteogenic medium. Statistical significant difference with respect to control or BMP-9 treated cells (*, **, ***).

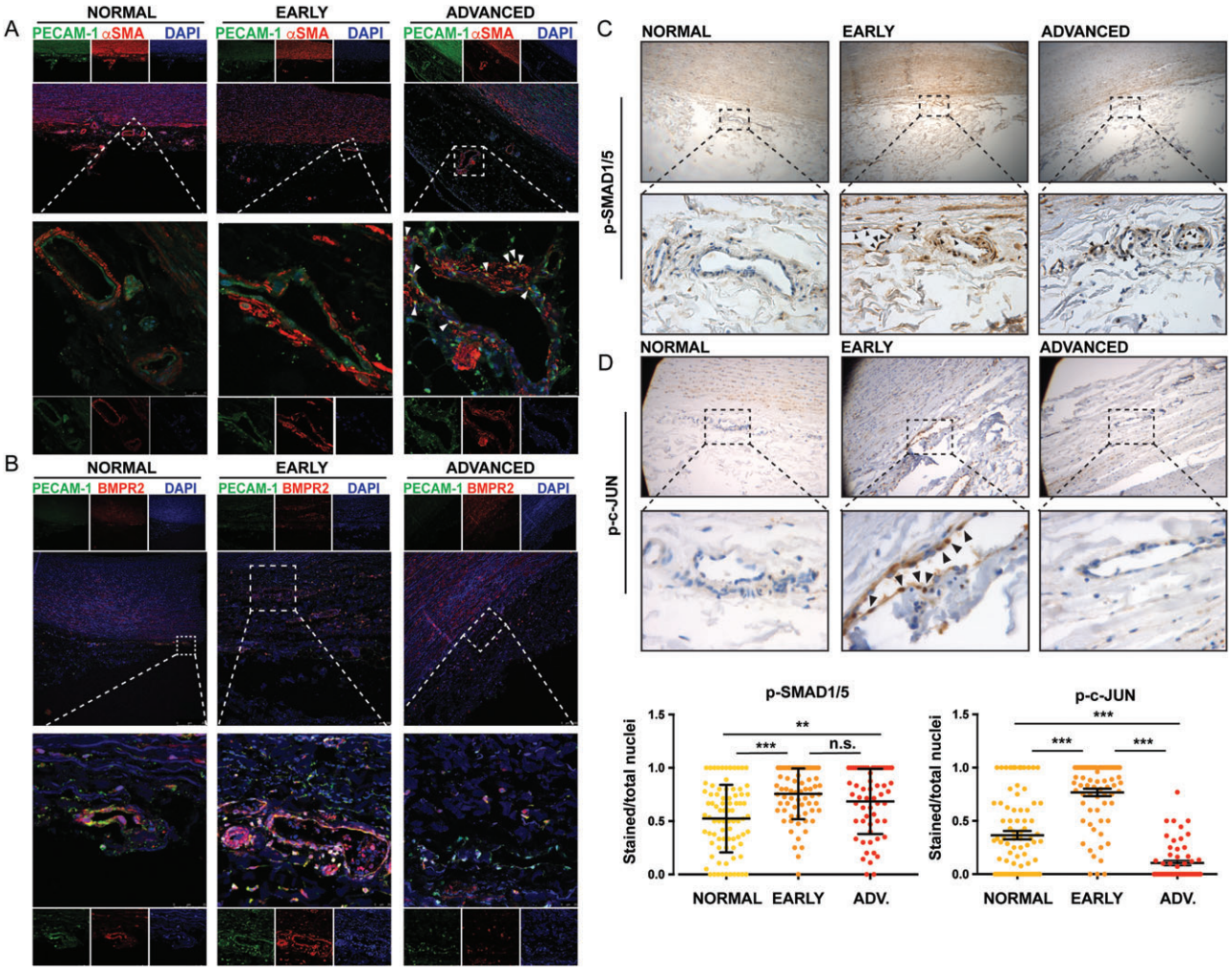

Figure 6. BMPR2 is downregulated in ECs of advanced lesions of human atherosclerosis. Immunofluorescent staining on aortic sections of control, early fibroatheroma (early), and fibrotic calcified plaque (FCP) donors. A representative picture per condition is shown. Zoomed images focus on microcapillaries in intimal and medial regions underneath the fibrotic core. (A) Staining for PECAM-1 (green), αSMA (red), and DAPI nuclear counterstain (blue). White arrows indicate PECAM-1/αSMA double-positive cells. (B) Staining for PECAM-1 (green), BMPR2 (red), and DAPI (blue). Immunohistochemical staining for p-SMAD1/5 (C) and p-c-Jun (D) on the aforementioned sections. Black arrows indicate positively stained cells. Low magnification (10×) and zoomed images (40×) are shown. (E) Quantification of C and D based on the numbers of p-SMAD1/5 or p-c-Jun-positive EC nuclei in one vessel/total nuclei in that vessel. A minimum of 55 vessels from three independent donors were considered per condition. Statistical significant difference between analyzed groups (**, ***).

ECs forming the vasa vasora in advanced human atherosclerosis exhibit reduced BMPR2 expression and JNK activation

A unique characteristic of human atherosclerosis is the progressive ingrowth of microcapillaries from the adventitia towards the intima layer in the aorta. We have previously shown that ECs lining such capillaries (known as *vasa vasora*) increase the expression of the transcription factor SLUG in the early stages of atherosclerosis [3], suggesting that these cells may undergo EndMT and thereby contribute to a population of cells with osteogenic potential. To further extend these studies, we performed immunofluorescent labeling on sections of human aorta corresponding to different stages of the atherosclerosis spectrum [34]. We observed an accumulation of αSMA-positive cells and loss of luminal PECAM-1 in microcapillaries from sections corresponding to fibrotic calcified plaque (advanced) (Figure 6A). Notably, we found double-positive PECAM-1/αSMA cells around the luminal endothelium, which is suggestive of EndMT. Furthermore, whereas BMPR2 was very potently expressed in ECs from capillaries of normal and early fibroatheroma (early) sections (Figure 6B), ECs in advanced lesions were very poorly stained for BMPR2 and PECAM-1. Finally, we analyzed the nuclear levels of p-SMAD1/5 and p-c-Jun in vasa vasorum ECs (Figure 6C,D). As Figure 6E shows, p-SMAD1/5 was significantly augmented in the ECs of early lesions and remained elevated in advanced lesions. On the contrary, p-c-Jun staining peaked in early stages and dramatically dropped in advanced lesions, in agreement with the loss of BMPR2. Altogether, these results support the mechanisms that we have identified *in vitro*, and propose BMPR2 as a novel biomarker and druggable target for human atherosclerosis.

Discussion

The identification of patients at increased risk of acute coronary events associated with vascular calcification, who may benefit from intensified preventative measures and for monitoring therapeutic efficacy, is a major ongoing challenge [46]. Recent publications have suggested that ECs directly contribute to vascular calcification through EndMT [2–4,42]. We investigated the interplay between inflammatory cytokines and BMPs, a subfamily of the TGF-β family, in ECs. We found that the pro-inflammatory cytokine TNF-α induces EndMT in HAoECs, thereby enhancing their differentiation into osteoblast-like cells in response to BMP-9. TNF-α and IL-1β induced EndMT in HAoECs, which results in BMPR2 downregulation. BMPR2 loss is sufficient and necessary for TNF-α to trigger EndMT in HAoECs. In addition, BMPR2 downregulation coincides with neointima formation and a decrease of luminal PECAM1-positive cells in ApoE3Leiden mice subjected to a high-fat diet. Moreover, we showed that in the absence of BMPR2, BMP-9 induces the formation of a receptor complex involving ACVR2A to induce downstream canonical signaling. Interestingly, we identified that BMPR2 downregulation leads to decreased JNK activation in ECs, as measured by phosphorylation of its downstream target c-Jun, and we showed that JNK deactivation facilitates BMP-induced mineralization in ECs. Finally, we showed that adventitial microvessels (*vasa vasora*) in advanced atherosclerotic disease exhibit loss of luminal PECAM1 and BMPR2 and accumulation of PECAM1/αSMA double-positive cells in layers underneath, suggestive of EndMT. Congruently, whereas p-SMAD1/5 increases in *vasa vasora* ECs at early stages of atherosclerosis and remains sustained in advanced lesions, p-c-Jun activation drops dramatically in vessels in fibrotic calcified plaque lesions. These results point to a key role of BMPR2 as an integrator of TGF-β/BMP and inflammatory signaling in ECs, determining EndMT and subsequent calcification.

Endothelial cells with reduced BMPR2 expression displayed increased expression of inflammatory markers such as ICAM and VCAM [47]. Interestingly, siRNA-mediated knockdown of BMPR2 in human umbilical vein endothelial cells (HUVECs) led to reduced p-SMAD1/5 in response to BMP-4, although the authors did not test whether this effect was specific for BMPR2. BMP-9, unlike BMP-4, shows a high affinity for ALK1 in ECs [37] and BMPR2 [48], which may result in a different contribution of BMPR2 in BMP-9 or BMP-4-induced receptor complexes. Furthermore, ALK1 (and not ALK2) was recently shown to mediate LDL uptake in ECs [49], and exposure of ECs to an inflammatory cocktail lowered their LDL uptake capacity [50]. Whether BMPR2 deficiency alters the ALK1–LDL interaction is an interesting area of study.

BMPR2 deficiency leads to pulmonary arterial hypertension (PAH), where heterozygous germline mutations in the *BMPR2* gene are found in more than 70% of patients with hereditary PAH and in 20% of patients with idiopathic PAH [51,52]. Several publications have indicated EndMT as a causative factor for the vascular remodeling in the pulmonary arteries of PAH patients [53,54]. Furthermore, PAH patients display a higher tendency to develop calcified lesions within the pulmonary arteries [55], suggesting that BMPR2 may have a protective role by inhibiting calcification in cells with osteogenic potential. In this sense, osteoblast-specific knockout of *Bmpr2* led to increased bone mass in transgenic mice [56]. Importantly, BMP-9 has been recently proposed as a therapeutic option for PAH [12]. Nevertheless, it remains to be determined whether systemic administration of BMP-9 may lead to calcification of the arteries under inflammatory conditions, such as those considered risk factors for atherosclerotic disease (renal disease, diabetes, hypertension or hyperlipidemia).

In summary, we have shown that aortic ECs undergo EndMT in response to inflammatory stimuli, which favor the calcification of ECs. Dissection of the underlying mechanisms of such enhanced osteogenic potential suggests that non-canonical signal transduction fine-tunes BMP-SMAD1/5 signaling, thereby enhancing the osteogenic differentiation of ECs (summarized in the supplementay material, Figure S14). A hallmark of this process is the downregulation of BMPR2. Therefore, monitoring BMPR2 as a biomarker of calcification or developing drugs specifically increasing BMPR2 expression to prevent EndMT in the arteries constitutes an area of interest for future research.

Acknowledgements

We thank K Iwata, S Vukicevic, and J Nickel for reagents. We are grateful to Martijn Rabelink for shRNA lentiviral constructs. We thank Maarten van Dinther, Midory Thorikay, Kirsten Lodder, and Karien Weismeijer for excellent technical assistance, and the entire group for scientific discussions. Research in the laboratory of PTD and MJG on the TGF-β family is supported by grants from the Netherlands Cardiovascular Research Initiative: the Dutch Heart Foundation, Dutch Federation of University Medical Centres, the Netherlands Organization for Health Research and development and Development, and the Royal Netherlands Academy of Sciences (PHAEDRA Consortium), and by the gravitation program CancerGenomiCs.nl from the Netherlands Organization for Scientific Research (NWO). MJG and VP are supported by the BAV Consortium (2013T093). GSD is supported by the RECONNECT Consortium (belonging to the Netherlands Cardiovascular Research Initiative, as aforementioned) and a Postdoctoral Fellowship from AFM-Telethon. AGV would like to acknowledge the Dutch Arthritis Association (Reumafonds) for support.

Author contributions statement

GSD, PtD, JL, MJG, and MDV designed the study. GSD, AGVA, VP, STGJ, and MG collected the data. GSD,

AGVA, VP, STGJ, and MG analyzed the data. GSD, PtD, JL, MJG, HVD, and MDV interpreted the data. GSD, PtD, JL, MJG, HVD, and MDV searched the literature. GSD, AGVA, VP, and STGJ generated the figures. GSD, PtD, MJG, JL, HVD, and MDV wrote the manuscript.

Abbreviations

ALK, activin receptor-like kinase; ARS, alizarin red solution; αSMA, alpha smooth muscle actin; BMP, bone morphogenetic protein; BMPR, BMP receptor; EFA, early fibroatheroma; EndMT, endothelial-to-mesenchymal transition; FCP, fibrotic calcified plaque; OM, osteogenic medium; PAH, pulmonary arterial hypertension; SMAD, homolog of the *Drosophila* protein, mothers against decapentaplegic (MAD) and *C. elegans* protein SMA; VE-cadherin, vascular endothelial cadherin

References

1. Libby P, Ridker PM, Hansson GK. Progress and challenges in translating the biology of atherosclerosis. *Nature* 2011; **473:** 317–325.
2. Evrard SM, Lecce L, Michelis KC, *et al.* Endothelial to mesenchymal transition is common in atherosclerotic lesions and is associated with plaque instability. *Nat Commun* 2016; **7:** 1–15.
3. Sánchez-Duffhues G, de Vinuesa AG, Lindeman JH, *et al.* SLUG is expressed in endothelial cells lacking primary cilia to promote cellular calcification. *Arterioscler Thromb Vasc Biol* 2015; **35:** 616–627.
4. Chen P-Y, Qin L, Baeyens N, *et al.* Endothelial-to-mesenchymal transition drives atherosclerosis progression. *J Clin Invest* 2015; **125:** 4514–4528.
5. Sánchez-Duffhues G, García De Vinuesa A, ten Dijke P. Endothelial to mesenchymal transition in cardiovascular diseases: developmental signalling pathways gone awry. *Dev Dyn* 2018; **247:** 492–508.
6. Gisterå A, Hansson GK. The immunology of atherosclerosis. *Nat Rev Nephrol* 2017; **13:** 368–380.
7. Boström K, Watson KE, Horn S, *et al.* Bone morphogenetic protein expression in human atherosclerotic lesions. *J Clin Invest* 1993; **91:** 1800–1809.
8. Dhore CR, Cleutjens JP, Lutgens E, *et al.* Differential expression of bone matrix regulatory proteins in human atherosclerotic plaques. *Arterioscler Thromb Vasc Biol* 2001; **21:** 1998–2003.
9. Morrell NW, Bloch DB, ten Dijke P, *et al.* Targeting BMP signalling in cardiovascular disease and anaemia. *Nat Rev Cardiol* 2016; **13:** 106–120.
10. David L, Mallet C, Keramidas M, *et al.* Bone morphogenetic protein-9 is a circulating vascular quiescence factor. *Circ Res* 2008; **102:** 914–922.
11. van Meeteren LA, Thorikay M, Bergqvist S, *et al.* Anti-human activin receptor-like kinase 1 (ALK1) antibody attenuates bone morphogenetic protein 9 (BMP9)-induced ALK1 signaling and interferes with endothelial cell sprouting. *J Biol Chem* 2012; **287:** 18551–18561.
12. Long L, Ormiston ML, Yang X, *et al.* Selective enhancement of endothelial BMPR-II with BMP9 reverses pulmonary arterial hypertension. *Nat Med* 2015; **21:** 777–785.
13. Mitrofan C-G, Appleby SL, Nash GB, *et al.* Bone morphogenetic protein 9 (BMP9) and BMP10 enhance tumor necrosis factor-α-induced monocyte recruitment to the vascular endothelium mainly via activin receptor-like kinase 2. *J Biol Chem* 2017; **292:** 13714–13726.
14. Kang Q, Sun MH, Cheng H, *et al.* Characterization of the distinct orthotopic bone-forming activity of 14 BMPs using recombinant adenovirus-mediated gene delivery. *Gene Ther* 2004; **11:** 1312–1320.
15. Saeed O, Otsuka F, Polavarapu R, *et al.* Pharmacological suppression of hepcidin increases macrophage cholesterol efflux and reduces foam cell formation and atherosclerosis. *Arterioscler Thromb Vasc Biol* 2012; **32:** 299–307.
16. Derwall M, Malhotra R, Lai CS, *et al.* Inhibition of bone morphogenetic protein signaling reduces vascular calcification and atherosclerosis. *Arterioscler Thromb Vasc Biol* 2012; **32:** 613–622.
17. de Vinuesa AG, Abdelilah-Seyfried S, Knaus P, *et al.* BMP signaling in vascular biology and dysfunction. *Cytokine Growth Factor Rev* 2016; **27:** 65–79.
18. de Jong DS, Vaes BLT, Dechering KJ, *et al.* Identification of novel regulators associated with early-phase osteoblast differentiation. *J Bone Miner Res* 2004; **19:** 947–958.
19. Zhang YE. Non-Smad pathways in TGF-β signaling. *Cell Res* 2009; **19:** 128–139.
20. Mu Y, Gudey SK, Landström M. Non-Smad signaling pathways. *Cell Tissue Res* 2012; **347:** 11–20.
21. Gilbert L, He X, Farmer P, *et al.* Inhibition of osteoblast differentiation by tumor necrosis factor-alpha. *Endocrinology* 2000; **141:** 3956–3964.
22. Kaneki H, Guo R, Chen D, *et al.* Tumor necrosis factor promotes Runx2 degradation through up-regulation of Smurf1 and Smurf2 in osteoblasts. *J Biol Chem* 2006; **281:** 4326–4333.
23. Gerstenfeld LC, Cho TJ, Kon T, *et al.* Impaired fracture healing in the absence of TNF-alpha signaling: the role of TNF-alpha in endochondral cartilage resorption. *J Bone Miner Res* 2003; **18:** 1584–1592.
24. Chang J, Wang Z, Tang E, *et al.* Inhibition of osteoblastic bone formation by nuclear factor-κB. *Nat Med* 2009; **15:** 682–689.
25. De Boeck M, Cui C, Mulder AA, *et al.* Smad6 determines BMP-regulated invasive behaviour of breast cancer cells in a zebrafish xenograft model. *Sci Rep* 2016; **6:** 24968.
26. Tasev D, van Wijhe MH, Weijers EM, *et al.* Long-term expansion in platelet lysate increases growth of peripheral blood-derived endothelial-colony forming cells and their growth factor-induced sprouting capacity. *PLoS One* 2015; **10:** e0129935.
27. O'Connell KA, Rudmann AA. Cloned spindle and epithelioid cells from murine Kaposi's sarcoma-like tumors are of endothelial origin. *J Invest Dermatol* 1993; **100:** 742–745.
28. O'Connell K, Landman G, Farmer E, *et al.* Endothelial cells transformed by SV40 T antigen cause Kaposi's sarcomalike tumors in nude mice. *Am J Pathol* 1991; **139:** 743–749.
29. Zhang J, Zhang X, Zhang L, *et al.* LRP8 mediates Wnt/β-catenin signaling and controls osteoblast differentiation. *J Bone Miner Res* 2012; **27:** 2065–2074.
30. van Dinther M, Visser N, de Gorter DJJ, *et al.* ALK2 R206H mutation linked to fibrodysplasia ossificans progressiva confers constitutive activity to the BMP type I receptor and sensitizes mesenchymal cells to BMP-induced osteoblast differentiation and bone formation. *J Bone Miner Res* 2010; **25:** 1208–1215.
31. Hamdi M, Kool J, Cornelissen-Steijger P, *et al.* DNA damage in transcribed genes induces apoptosis via the JNK pathway and the JNK-phosphatase MKP-1. *Oncogene* 2005; **24:** 7135–7144.
32. Lardenoye JHP, de Vries MR, Löwik CWGM, *et al.* Accelerated atherosclerosis and calcification in vein grafts: a study in APOE*3 Leiden transgenic mice. *Circ Res* 2002; **91:** 577–584.
33. Virmani R, Kolodgie FD, Burke AP, *et al.* Lessons from sudden coronary death: a comprehensive morphological classification

scheme for atherosclerotic lesions. *Arterioscler Thromb Vasc Biol* 2000; **20:** 1262–1275.
34. van Dijk RA, Virmani R, von der JH T, *et al.* The natural history of aortic atherosclerosis: a systematic histopathological evaluation of the peri-renal region. *Atherosclerosis* 2010; **210:** 100–106.
35. Korchynskyi O, ten Dijke P. Identification and functional characterization of distinct critically important bone morphogenetic protein-specific response elements in the Id1 promoter. *J Biol Chem* 2002; **277:** 4883–4891.
36. Rennefahrt UEE, Illert B, Kerkhoff E, *et al.* Constitutive JNK activation in NIH 3T3 fibroblasts induces a partially transformed phenotype. *J Biol Chem* 2002; **277:** 29510–29518.
37. Scharpfenecker M, van Dinther M, Liu Z, *et al.* BMP-9 signals via ALK1 and inhibits bFGF-induced endothelial cell proliferation and VEGF-stimulated angiogenesis. *J Cell Sci* 2007; **120:** 964–972.
38. Rosenzweig BL, Imamura T, Okadome T, *et al.* Cloning and characterization of a human type II receptor for bone morphogenetic proteins. *Proc Natl Acad Sci U S A* 1995; **92:** 7632–7636.
39. Ichijo H, Yamashita H, ten Dijke P, *et al.* Characterization of *in vivo* phosphorylation of activin type II receptor. *Biochem Biophys Res Commun* 1993; **194:** 1508–1514.
40. ten Dijke P, Yamashita H, Ichijo H, *et al.* Characterization of type I receptors for transforming growth factor-β and activin. *Science* 1994; **264:** 101–104.
41. Upton PD, Morrell NW. TGF-β and BMPR-II pharmacology – implications for pulmonary vascular diseases. *Curr Opin Pharmacol* 2009; **9:** 274–280.
42. Guihard PJ, Yao J, Blazquez-Medela AM, *et al.* Endothelial–mesenchymal transition in vascular calcification of $Ins2^{Akita/+}$ mice. *PLoS One* 2016; **11:** e0167936.
43. Wang L, Luo J-Y, Li B, *et al.* Integrin-YAP/TAZ-JNK cascade mediates atheroprotective effect of unidirectional shear flow. *Nature* 2016; **540:** 579–582.
44. Podkowa M, Zhao X, Chow C-W, *et al.* Microtubule stabilization by bone morphogenetic protein receptor-mediated scaffolding of c-Jun N-terminal kinase promotes dendrite formation. *Mol Cell Biol* 2010; **30:** 2241–2250.
45. Chen W-K, Yeap YYC, Bogoyevitch MA. The JNK1/JNK3 interactome – contributions by the JNK3 unique N-terminus and JNK common docking site residues. *Biochem Biophys Res Commun* 2014; **453:** 576–581.
46. Franco M, Cooper RS, Bilal U, *et al.* Challenges and opportunities for cardiovascular disease prevention. *Am J Med* 2011; **124:** 95–102.
47. Kim CW, Song H, Kumar S, *et al.* Anti-inflammatory and antiatherogenic role of BMP receptor II in endothelial cells. *Arterioscler Thromb Vasc Biol* 2013; **33:** 1350–1359.
48. Kraehling JR, Chidlow JH, Rajagopal C, *et al.* Genome-wide RNAi screen reveals ALK1 mediates LDL uptake and transcytosis in endothelial cells. *Nat Commun* 2016; **7:** 1–15.
49. Rieder F, Kessler SP, West GA, *et al.* Inflammation-induced endothelial-to-mesenchymal transition: a novel mechanism of intestinal fibrosis. *Am J Pathol* 2011; **179:** 2660–2673.
50. Brown MA, Zhao Q, Baker KA, *et al.* Crystal structure of BMP-9 and functional interactions with pro-region and receptors. *J Biol Chem* 2005; **280:** 25111–25118.
51. International PPH Consortium, Lane KB, Machado RD, *et al.* Heterozygous germline mutations in *BMPR2*, encoding a TGF-β receptor, cause familial primary pulmonary hypertension. *Nat Genet* 2000; **26:** 81–84.
52. Deng Z, Morse JH, Slager SL, *et al.* Familial primary pulmonary hypertension (gene *PPH1*) is caused by mutations in the bone morphogenetic protein receptor-II gene. *Am J Hum Genet* 2000; **67:** 737–744.
53. Ranchoux B, Antigny F, Rucker-Martin C, *et al.* Endothelial-to-mesenchymal transition in pulmonary hypertension. *Circulation* 2015; **131:** 1006–1018.
54. Qiao L, Nishimura T, Shi L, *et al.* Endothelial fate mapping in mice with pulmonary hypertension. *Circulation* 2014; **129:** 692–703.
55. Ruffenach G, Chabot S, Tanguay VF, *et al.* Role for runt-related transcription factor 2 in proliferative and calcified vascular lesions in pulmonary arterial hypertension. *Am J Respir Crit Care Med* 2016; **194:** 1273–1285.
56. Lowery JW, Intini G, Gamer L, *et al.* Loss of BMPR2 leads to high bone mass due to increased osteoblast activity. *J Cell Sci* 2015; **128:** 1308–1315.
*57. Nakao A, Imamura T, Souchelnytskyi S, *et al.* TGF-β receptor-mediated signalling through Smad2, Smad3 and Smad4. *EMBO J* 1997; **16:** 5353–5362.
*58. Zou Y, Dietrich H, Hu Y, *et al.* Mouse model of venous bypass graft arteriosclerosis. *Am J Pathol* 1998; **153:** 1301–1310.
*59. LJAC H, Paauwe M, Verspaget HW, *et al.* Interaction with colon cancer cells hyperactivates TGF-β signaling in cancer-associated fibroblasts. *Oncogene* 2014; **33:** 97–107.

*Cited only in supplementary material.

SUPPLEMENTARY MATERIAL ONLINE

Supplementary materials and methods

Supplementary figure legends

Figure S1. TNF-α and IL-1β induce the upregulation of EndMT factors in HAoECs

Figure S2. Long-term effect of TNF-α and TGF-β in HAoECs

Figure S3. TNF-α and IL-1β induce the downregulation of *BMPR2* in HAoECs

Figure S4. TNF-α induces the upregulation of BMPR2 in a cell type-specific manner

Figure S5. TNF-α downregulates BMPR2 in a dose-dependent manner

Figure S6. BMP receptor activation is required to induce cell mineralization in 2H-11 endothelial cells

Figure S7. *Bmpr2* knockdown enhances BMP-9-induced mineralization in 2H-11 cells

Figure S8. Knockdown of *Acvr2A* or *Acvr2B* does not affect BMP-9-induced mineralization in 2H-11 cells

Figure S9. *Bmpr2* overexpression partially prevents BMP-9-induced mineralization in 2H-11 cells